Toward Brain-Actuated Humanoid Robots: Asynchronous Direct Control Using an EEG-Based BCI

Yongwook Chae, Jaeseung Jeong, Sungho Jo

IEEE Transactions on Robotics.(2012.10)

Presenter : Soogil Woo

GIST, Dept. of Information and Communication, INFONET Lab.

Gwangju Institute of
Science and Technology

Introduction

- In the past, there have been numerous attempts to design and build full-bodied humanoid robots.

- The realization of a robotic system that understands human intentions and produces complex behaviors is needed, for disabled or elderly persons.

- The EEG-based BCI system for robots has been suggested in robotics and neural engineering fields because some elderly or disabled people can control robots naturally and intuitively by thinking while using this system.

- The active BCI can control an application using consciously intended brain signals without external events.

- BCI methods using sensorimotor rhythms belong to the active BCI.

- These methods classify specific motor images in a general sense through the power over the frequency ranges [e.g., mu (8–12 Hz) or beta (18–22 Hz)].

Introduction

- In a synchronous BCI system, sequential cues are provided at a fixed rate.

- Because a user cannot control the timing of motion commands, it tends to lower the information transfer rate (ITR).

- One main goal of EEG-based BCIs for human robot interaction is being able to command a robot directly by thinking.

- This paper describes a new brain-actuated humanoid robot navigation system that allows for asynchronous direct control of humanoid motions using the active BCI system.

- Their system provides five low-level motion commands (e.g., "stop," "turn the head to the left," "turn the head to the right," "turn the body," or "walk forward") by combining the classification of three motor imagery (MI) states (e.g., "left hand," "right hand," or "foot") with a posture-dependent control paradigm.

- To evaluate the proposed system, a humanoid robot navigation experiment in a maze was conducted with human subjects.

Methods

- Their proposed system has four key features.

- First, low-level commands make the humanoid turn at any angle and walk to any position.

- Second, five complex humanoid motions are controlled by three intentional mental states.

- Third, the subject can command the humanoid using asynchronous protocol.

- Fourth, their system does not employ a reactive but rather an active system.

Methods(System Description)

- The system consists of three main subsystems: the BCI system, the interface system, and the humanoid control systems.

- The BCI system classifies four user mental states.

- The non-control state is referred to as "rest" and the three MI states are referred to as "left hand", "right hand", and "foot".
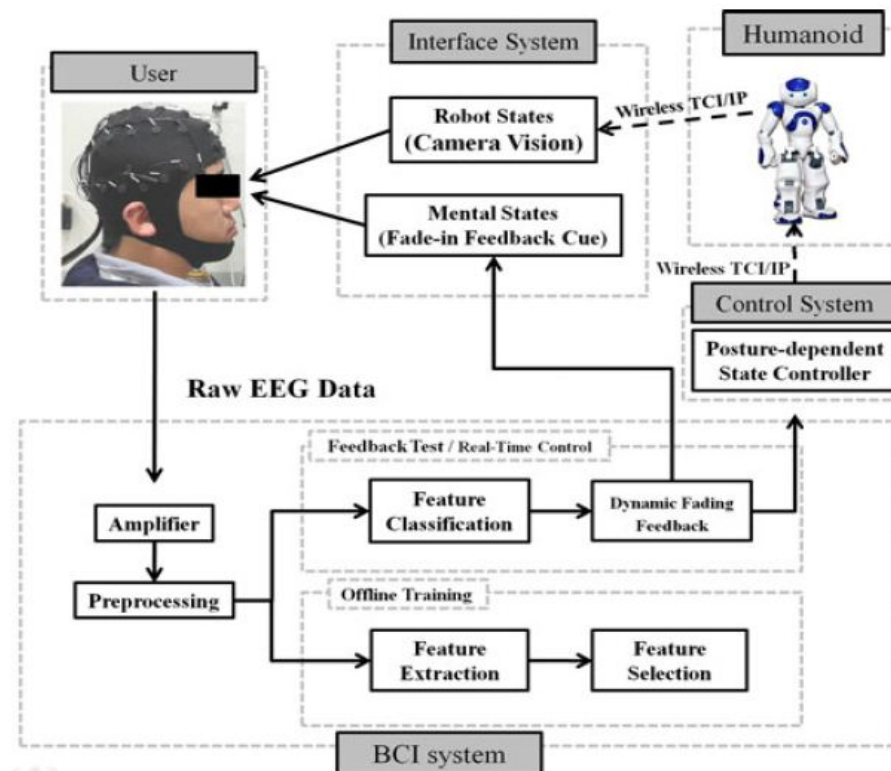
Methods(Experimental Protocol)

- 1) Offline training session

- 2) Selection of informative feature components and training of two classifiers

- 3) Online testing sessions

- 4) Checking the accuracy of the online session

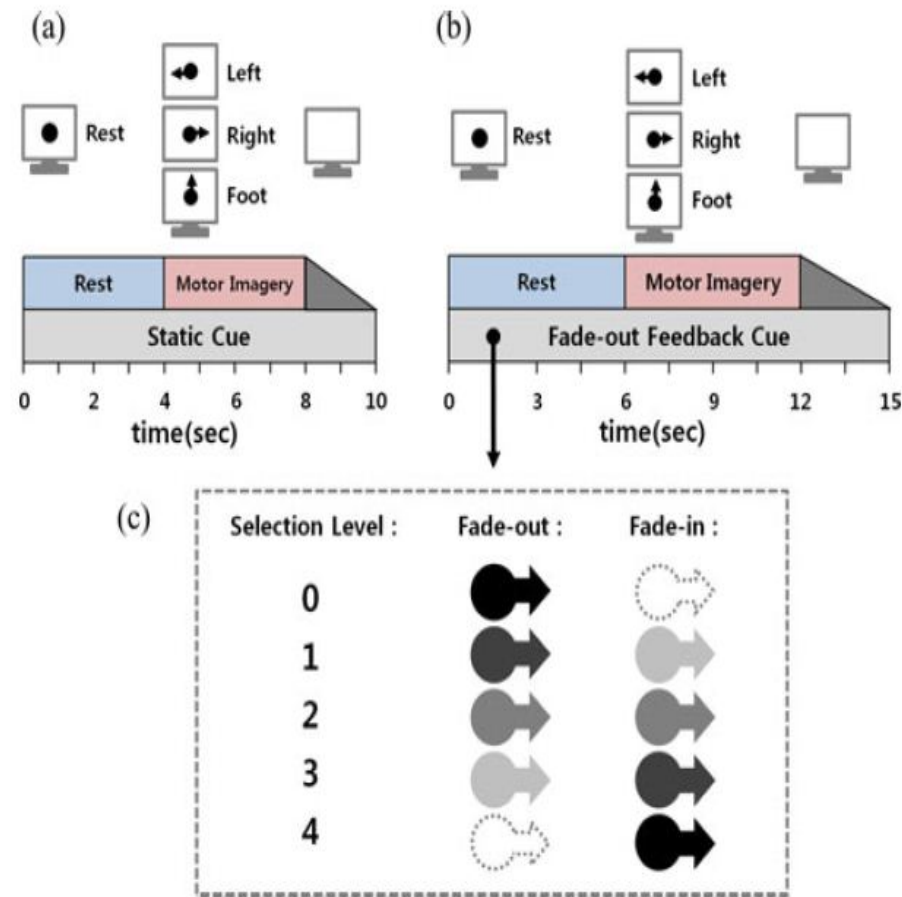- 5) Real-time humanoid navigation control experiment

Fig. 2. (a) Offline training protocol: After the rest sessions, the subject is asked to imagine a motor imagery indicated by a static cue. (b) Online feedback testing protocol: 6 s are allowed to test the performance of the classification with dynamic fade-out feedback. (c) Dynamic fading feedback is used to secure a robust classification of a mental state from the ongoing EEG (see Section II-H).

Methods(Experimental Protocol)

- To verify the navigation performance of system, an indoor maze was designed.

- It was aimed to reduce the bias through an order of experiments (manual control or BCI control).

- If they missed any waypoints, they could skip them.

- Each subject conducted the experiment 3 times using the BCI system and one time through keyboard control for comparison.
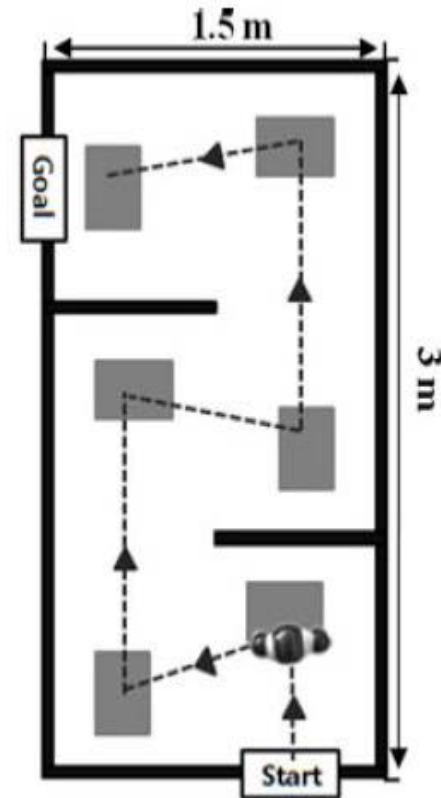
(a)   (b)

Methods(Data acquisition & Feature Extraction)

- In this paper, they applied this signal processing protocol to filter and detect the sensorimotor rhythm.

- An electrode at the vertex of the head was used as a reference, and extra electrode was used as a ground.

- The impedances of all of the electrodes were lower than 5 kΩ.

- For the real-time process, a total of 21 electrodes around the sensorimotor cortex were used to apply the large Laplacian filter over the nine frontocentroparietal locations based on the international 10-20 system as show in fig.
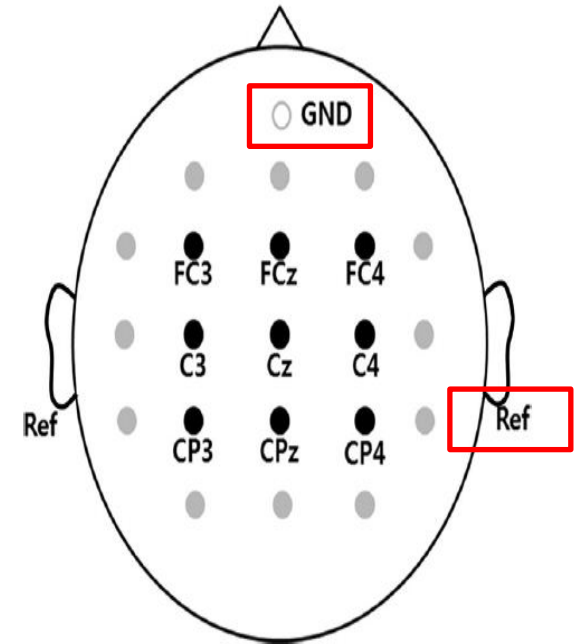

Fig. 4. EEG electrode positions with respect to the international 10–20 system. Electrode positions marked with gray circles were only used to compute the spatial filter. The nine black circles indicate the electrode positions used as the main feature channels. All electrodes are referenced to the left and right mastoids.

Methods(Data acquisition & Feature Extraction)

- To extract amplitude features, every 250ms observation segment recorded for 2 s (500 samples) from nine channels was analyzed by the autoregressive algorithm, and the square root of power in 1Hz wide frequency bands within 4-36 Hz was calculated.

- In the offline training session, 32 feature vectors with 288 dimensions (9 channels * 32 frequency components) were collected within the MI and rest periods (4 s for each) for one trial.

- These feature vectors were used to select informative feature components and train the classifiers.

- During the online testing and real-time control session, the feature vectors were sampled from the selected informative feature components and these were used to produce real-time feedback and classification for the motion commands.

Methods(Feature Selection)

- In this study, the Fisher ratio was used to select informative feature components of each subject that can be interpreted as suitable channel–frequency bands.

- For the amplitude feature vector from the "rest" and MI states, let μ_{rest} and σ_{rest} denote the mean and variance, respectively, of the amplitude feature set from the "rest" state, and let μ_{MI} and σ_{MI} denote the mean and variance, respectively, of the amplitude feature set from the MI state.

- The Fisher ratio is defined as the ratio of the between-class variance to the within-class variance as follows:

$$fr = \frac{\sigma^2_{between}}{\sigma^2_{within}} = \frac{\left(\mu_{rest} - \mu_{MI}\right)^2}{\sigma^2_{rest} + \sigma^2_{MI}}$$

- The Fisher ratio is a measure of the (linear) discrimination of two variables, and it can also be considered as a signal-to-noise ratio.
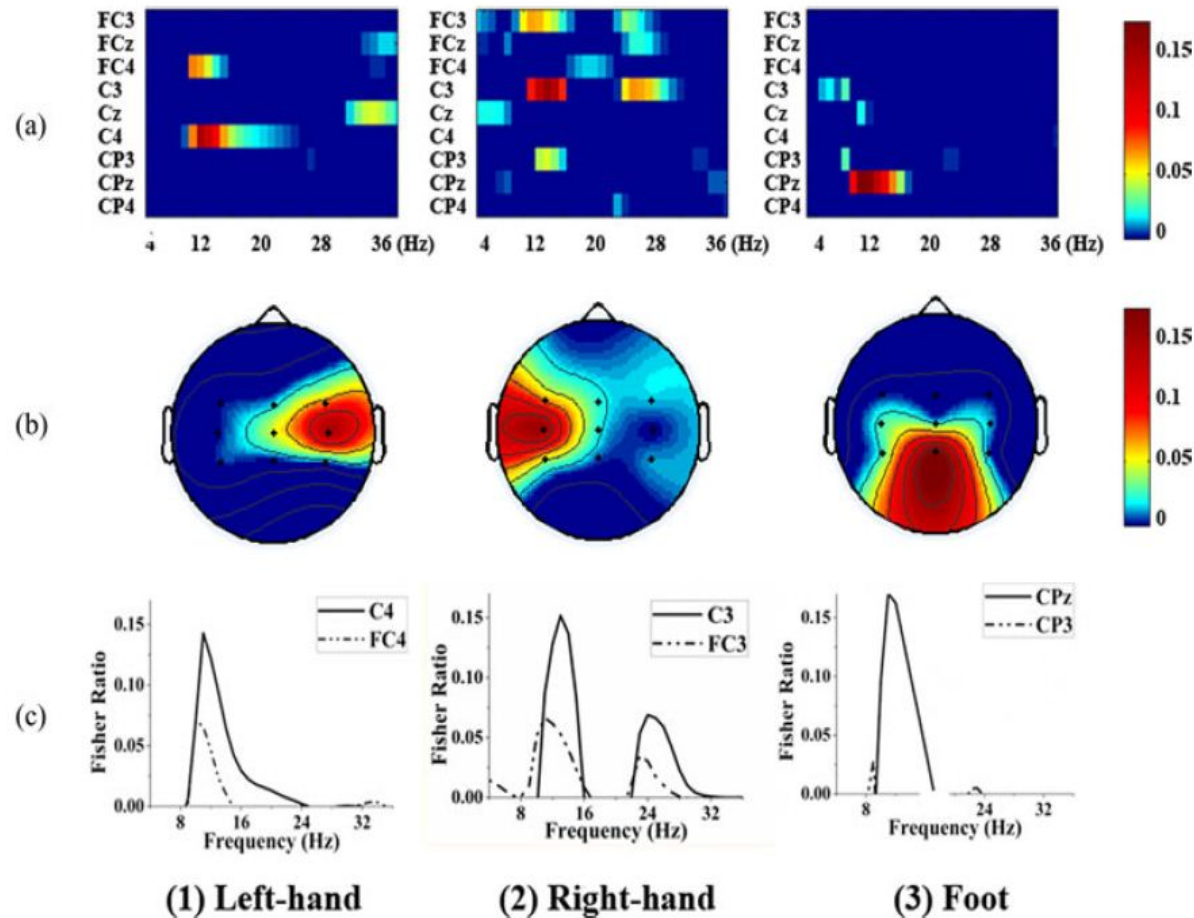
Methods(Feature Selection)

Fig. 5.   Channel–frequency selection using the Fisher ratios from three sets of "rest" versus MI tasks. (a) Channel–frequency distribution of the Fisher ratios of subject A. (b) Topographical distribution of the Fisher ratios of subject A at the highest frequency bands (12, 14, and 10 Hz, respectively). The first two top-scoring channels for the "left-hand" imagery tasks were channels C4 and FC4, while channels C3 and FC3 were selected for the "right-hand" imagery tasks, and channels CPz and Cz were selected for the "foot" imagery tasks. (c) Spectral distribution of the Fisher ratios for subject A. For the "left-hand" imagery tasks, the maximum Fisher ratio of C4 was 0.15 at 12 Hz, and a 5-Hz window centered at 12 Hz was selected as the optimal frequency region.

Methods(Classification)

- To translate the intended EEG data into appropriate movement commands for the humanoid robot, the intentional activity classifier (IAC) and movement direction classifier (MDC) were employed.

- If the signals are interpreted as the MI state by the IAC, then the MDC classifies the specific MI state as either a "left hand", "right hand", or "foot" states.

- For the initial training, the features from the training trials between 0 and 4 s (e.g., rest period) were assigned to the "rest" class, and the signal segments between 4 and 8 s (e.g., MI period) were assigned to the MI class.

- For the training, the negative output values of the IAC denote the "rest" classes, while the positive output values of the IAC denote the MI classes.

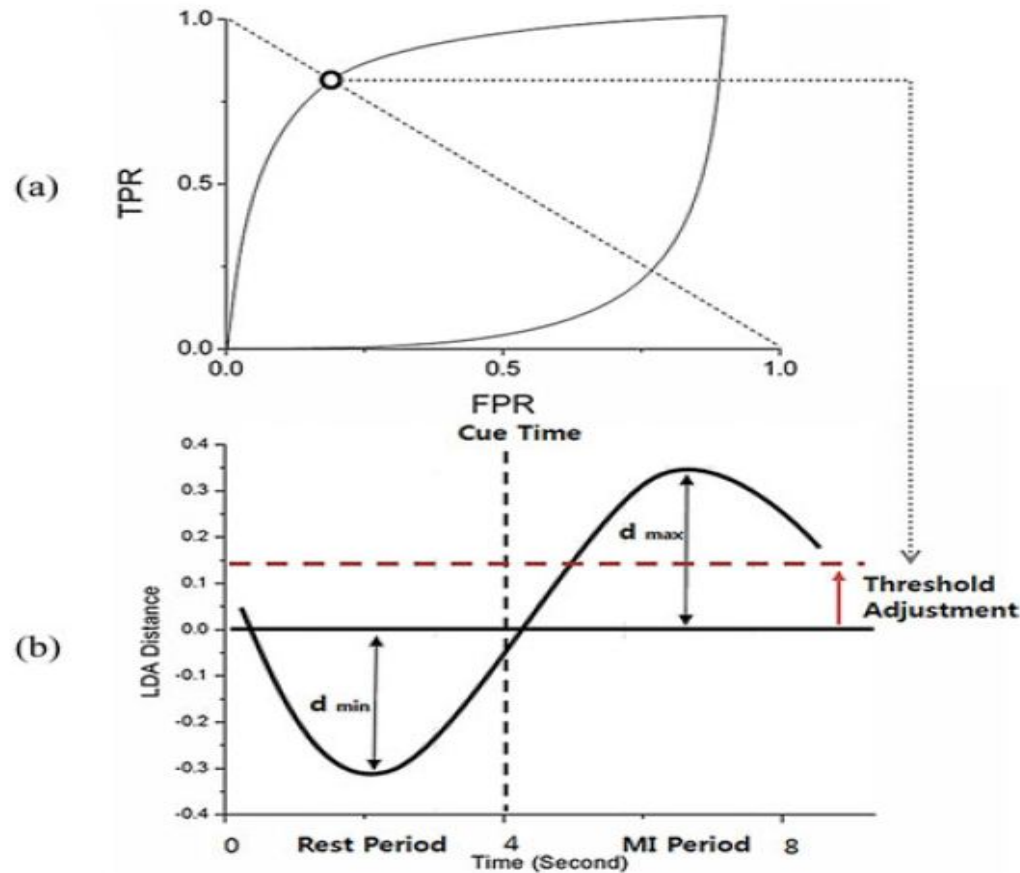# Methods(Classification)

Fig. 6.   Time period selection using the LDA distance metric and determination of a classifier threshold. (a) ROC curve determines an appropriate threshold value and (b) a typical intention level curve of a subject to discriminate the rest and MI time periods. As the informative time period, a 1-s interval centered at the maximum and minimum LDA distance points was selected.

Methods(Dynamic Fading Feedback rule)

- Because the classification results of the sensorimotor rhythm based active BCI could generate the misclassification results, some normalization methods would be used to enable a smooth transition between class-specific feedbacks.

- In this study, the dynamic fading feedback rule was designed to avoid abrupt false classifications, as shown in fig.
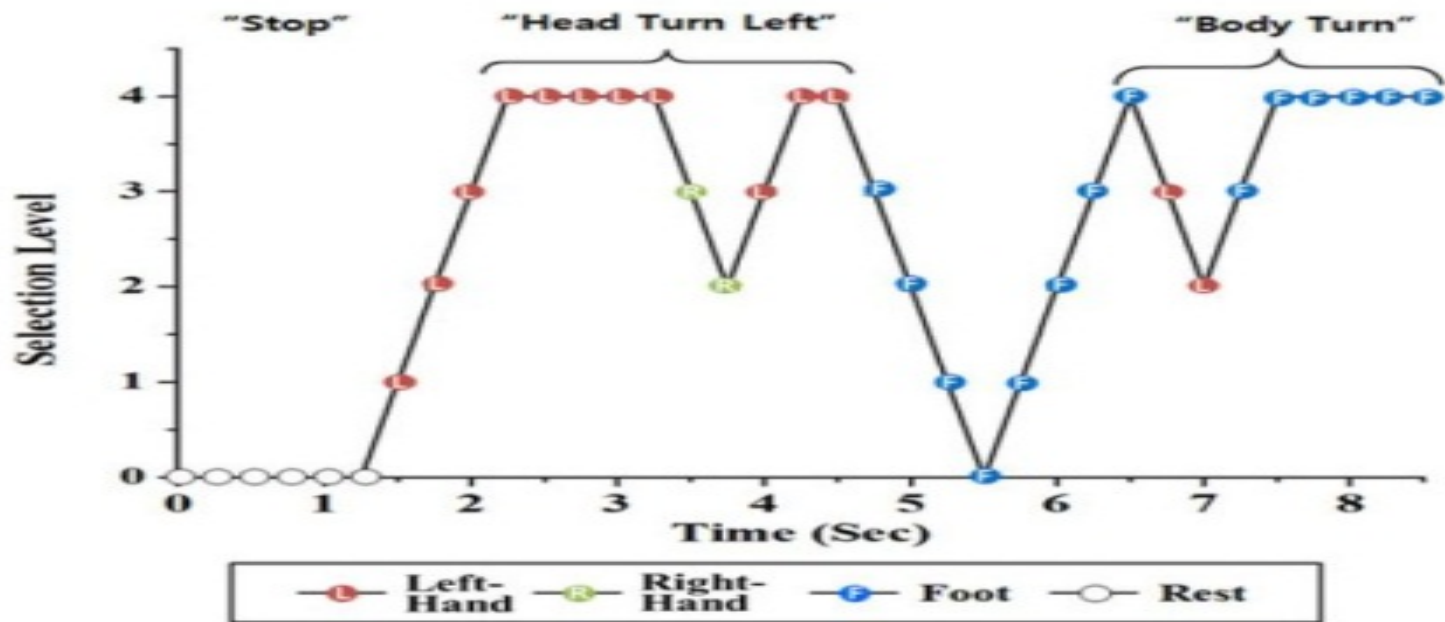

Fig. 8.   Dynamic fading feedback rule. Variation of selection levels and classifications of a real-time BCI experiment over 8.5 s.

Methods(Dynamic Fading Feedback rule)

- 1) the candidate decision produced during the online feedback testing session and the real-time control session

- 2) the selection level associated with the confidence measurement of selected classifications.

➢ Rule 1: When the selection level is zero, the next first classification is newly set to be the candidate's decision.

➢ Rule 2: Whenever the classification result is identical to the candidate decision, the selection level is increased by 1; otherwise, the selection level is decreased by 1.

➢ Rule 3: When the selection level reaches 4, the control system confirms its decision and generates a motion command accordingly (i.e., "left," "right," or "forward").

➢ Rule 4: The fading feedback cues and the arrow and text shown on the display are transparentized according to the candidate's decision and its selection level.

Methods(Dynamic Fading Feedback rule)

- Fig. 8 illustrates an example of the command selection procedure.

- For the first 1 s, the consecutive "rest" commands appear.

- At 1.25 s, the four consecutive "left-hand" classifications increase the selection level up to 4, and then, the system generates a "left" command. The robot executes its motion accordingly through the control paradigm, as described in Fig. 7 (i.e., "head turn left").

- Next, consecutive "left-hand" classifications cause the robot to keep turning its head to the left up to 15◦ (3◦ per command).
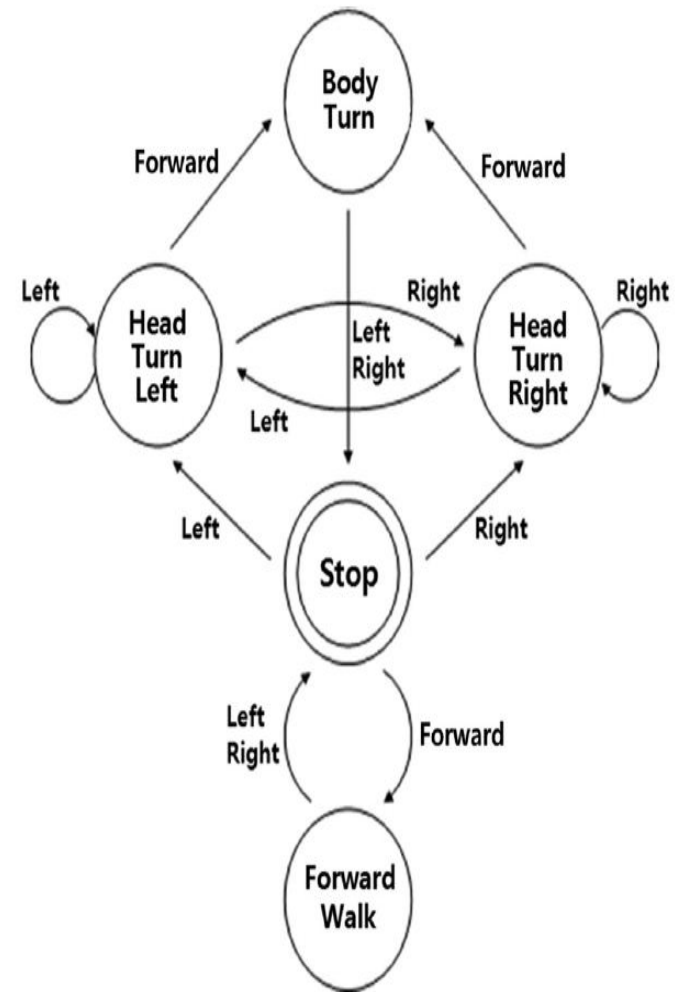

Fig. 7.   Diagram of humanoid navigation control. (Left) Left-hand imagery. (Right) Right-hand imagery. (Forward) Foot imagery.

Methods(Evaluation)

- 1) Performance of the Brain–Computer Interface System: (ITR)

$$I_d = \log_2 N + p \log_2 p + (1-p) \log_2 \{(1-p)/(N-1)\}, \quad \text{ITR} = f_d \times I_d$$

- I_d is the bit rate (bits/trial) for the three mental state choices (N=3), p is the accuracy, and f_d is the decision rate (trial/min).

- 2) Navigation Performance

- ✓ Total Time: total time taken to accomplish the task (in seconds);

- ✓ Traveled Distance: distance traveled to accomplish the task (in centimeters);

- ✓ Forward Steps: number of walking steps during forward movement;

- ✓ Turning Steps: number of walking steps to turn the robot body;

- ✓ Explored Angle: total turning angle of the robot head to explore the surrounding environment (in degrees);

- ✓ # Trans: number of transitions between the walking mode and the exploration mode;

- ✓ Waypoint: number of waypoints on which the robot

Results(Feature Selection)

- The Fisher ratios for the channel and frequency components and averaged discriminant values for the offline training period for each motor imagery and subject are illustrated.

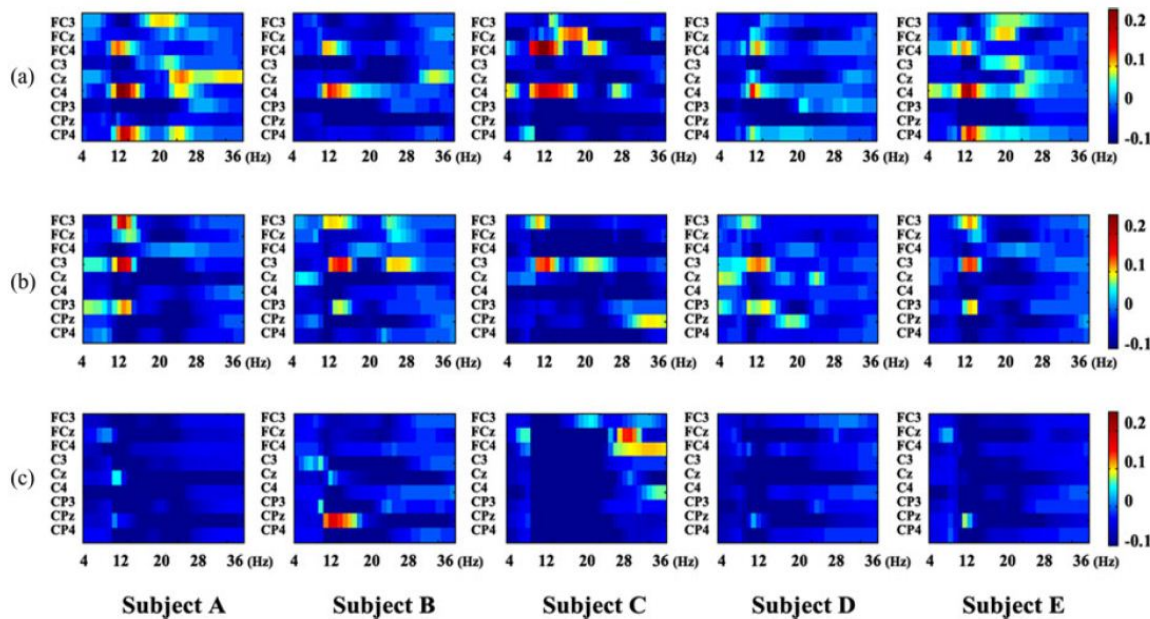- Table I describes the selected feature components of the five subjects.

Fig. 10. Channel–frequency distributions of Fisher ratios for all subjects for "left-hand," "right-hand," and "foot" imagery tasks. (a) Left. (b) Right. (c) Foot.

TABLE I
FEATURE SELECTION RESULTS

Subject	Left-hand Ch	Left-hand Freq	Right-hand Ch	Right-hand Freq	Foot Ch	Foot Freq
A	C4	9-13	FC3	10-14	Cz	8-12
	CP4	10-14	C3	9-13	CPz	7-11
B	C4	11-15	C3	12-16	CPz	10-14
	FC4	9-13	FC3	8-12	CP3	21-25
C	FC4	9-13	C3	9-13	FCz	26-30
	C4	10-14	FC3	7-11	FC4	28-32
D	C4	9-13	C3	10-13	CPz	8-12
	FC4	10-14	CP3	11-15	FC4	6-10
E	C4	9-13	C3	11-15	CPz	9-13
	CP4	10-14	FC3	11-15	FCz	6-10

Results(Navigation Performance)

- Tables II and III provide details about the performance of the two hierarchical classifiers (IAC and MDC) for the five subjects.

- Table II shows the number of offline training trials per mental task, the TPR and FPR of the IAC, and the accuracy of the MDC for each task.

- Table III shows the online testing performance achieved using the fading feedback rule for the given mental tasks.

TABLE II
OFFLINE TRAINING RESULTS

		A	B	C	D	E
Trials		140	160	120	200	200
Accuracy (%)	Left-hand	79.0	88.8	96.6	86.0	78.5
	Right-hand	85.9	89.4	82.0	62.3	74.0
	Foot	59.3	75.3	83.2	63.8	75.0
	Average	74.7	84.5	87.3	70.7	75.8
ITR (bit/min)		7.7	12.1	13.6	6.4	8.2

TABLE III
ONLINE FEEDBACK TESTING RESULTS

		A	B	C	D	E
Response Time (sec)	T1	2.2	1.6	1.4	1.9	2.1
	T2	3.4	3.1	2.6	3.5	3.3
Accuracy (%)	Left-hand	86.7	80.0	100.0	93.3	86.7
	Right-hand	80.0	86.7	93.3	66.7	66.7
	Foot	66.7	73.3	86.7	66.7	73.3
	Average	77.8	80.0	93.3	77.8	75.6
ITR (bit/min)		10.6	12.8	26.5	10.4	9.8

Results(Navigation Performance)

- The results of the real-time navigation experiments of the humanoid robot.

- During the manual control experiments, all of the subjects controlled the robot to pass through all five waypoints without any collisions during navigation.

- During the BCI control experiments, the robot stepped on 3.2 waypoints with an average of 0.3 collisions, while the robot always successfully reached the final position.

Subject	Session	Total time (sec)	Distance travelled (cm)	Forward steps (times)	Turning steps (times)	Explored angle (°)	# Trans. (times)	Waypoint (times)	Collisions (times)
A	BCI	634.1	335.5	102.7	64.3	1161.3	39.7	2.3	0.7
	Manual	479.7	415.8	126.0	64.0	543.0	27.0	5.0	0.0
B	BCI	642.4	429.0	129.3	78.3	1485.9	40	4	0.7
	Manual	432.7	403.7	129.0	58.0	501	21	5	0
C	BCI	632.3	430.1	130.3	69.7	974.0	49.7	4.7	0.0
	Manual	452.9	389.4	118.0	64.0	605.0	34.0	5.0	0.0
D	BCI	448.8	307.0	86.7	46.0	704.9	31.3	2.0	0.0
	Manual	410.5	481.0	134.0	61.0	494.1	21.0	5.0	0.0
E	BCI	448.8	410.0	115.0	51.7	585.1	27.0	2.7	0.3
	Manual	424.4	508.9	143.0	58.0	509.0	24.0	5.0	0.0
BCI	Mean	561.3	382.3	112.8	62.0	982.2	37.5	3.1	0.3
	(± Std)	(± 102.8)	(± 57.2)	(± 18.5)	(± 13.2)	(± 360.7)	(± 8.8)	(± 1.2)	(± 0.4)
Manual	Mean	440.0	439.8	130.0	61.0	530.4	25.4	5.0	0.0
	(± Std)	(± 27.0)	(± 52.2)	(± 9.3)	(± 3.0)	(± 45.7)	(± 5.4)	(± 0.0)	(± 0.0)

Results(Navigation Performance)

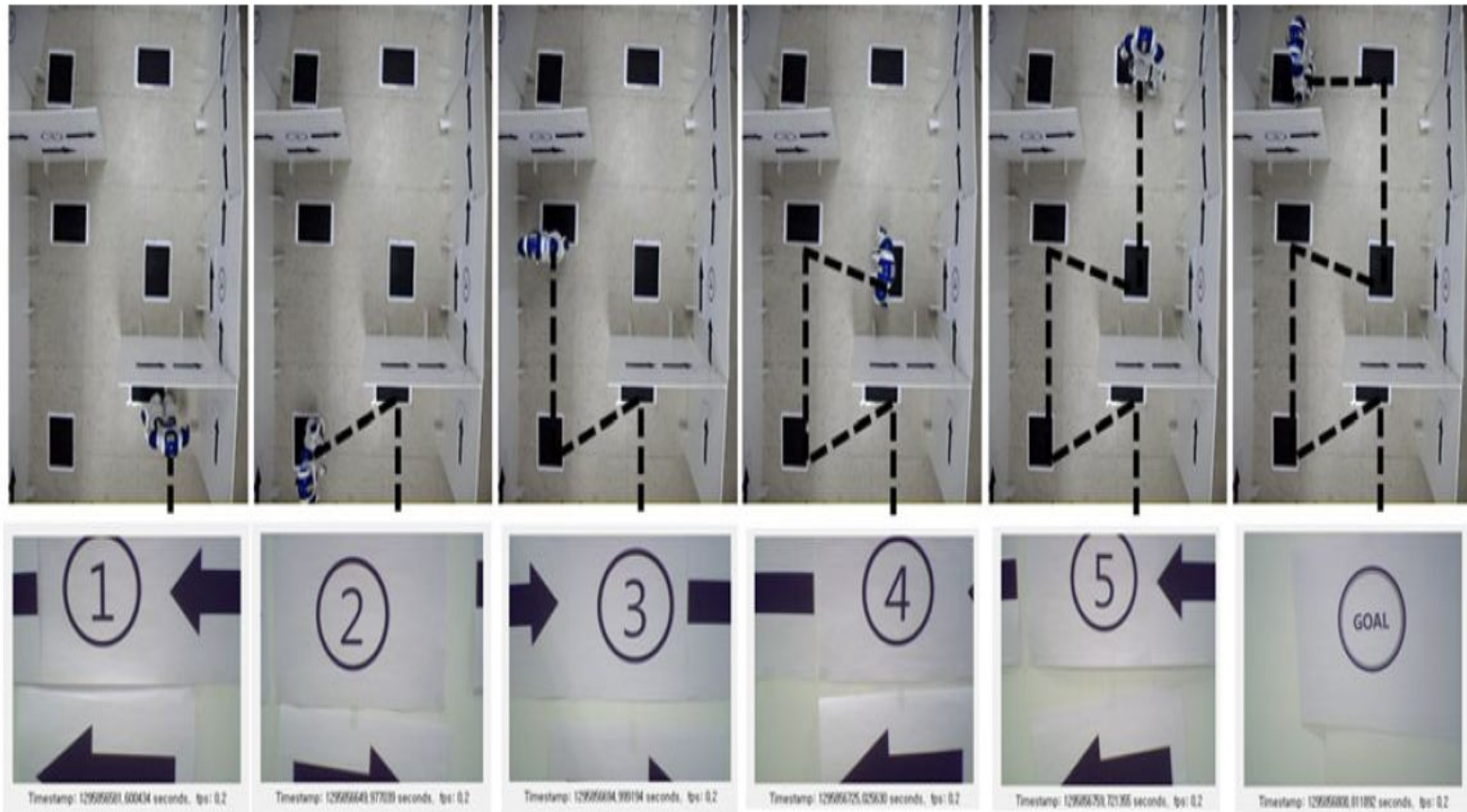- Fig. shows the sequential snapshots taken during an experiment.

Fig. 12. Navigation task is to make the robot move from a starting position to destination regions, while passing through the five waypoints at the corners of the maze. The first row shows snapshots taken during a trial, and the second row shows images acquired from the robot camera at each position.

Discussions

- This paper has described a new humanoid navigation system that is directly controlled through an asynchronous sensorimotor rhythm-based BCI system.

- Their approach allows for flexible robotic motion control in unknown environments using a camera vision.

- Brain-actuated humanoid control by this active BCI could be further improved in speed and accuracy.

- Recently, researchers have introduced hybrid BCIs that exploit the advantages of different reactive approaches (e.g., P300 or steady-state visually evoked potentials) and active approaches to improve the overall performance of BCI system.

- Another extension of this study is to realize human–robot interaction that can recognize high-level human cognitions, such as affective states.

Thank you!